The Dynamical Influence of Land–Sea Contrast and Sea Surface Temperature on Intraseasonal Oscillation in Tropical Atmosphere

Yang Yan (杨 燕) and *Zhu Baozhen* (朱抱真)
Institute of Atmospheric Physics, Chinese Academy of Sciences, Beijing, 100080
Received January 25, 1995; revised March 23, 1995

ABSTRACT

An equatorial β-plane model which includes realistic non-uniform land-sea contrast and the underlying surface temperature distribution is used to simulate the 30–60 day oscillation (LFO) processes in tropical atmosphere, with emphasis on its longitude-dependent evolution and convective seesaw between Indian and the western Pacific oceans.

The model simulated the twice-amplification of the disturbances over Indian and the western Pacific oceans while they are travelling eastward. It reproduced the dipole structure caused by the out-of-phase oscillation of the active centres in these two areas and the periodical transition between the phases of LFO. It is suggested that the convective seesaw is the result of interaction of the internal dynamics of tropical atmosphere with the zonally non-uniform thermal forcing from underlying surface. The convective activities are suppressed over Indonesia maritime continents whilst they are favoured over the Indian Ocean and western Pacific warm waters, so there formed two active oscillation centres. The feedback of convection with large-scale flow slows down the propagation of disturbances when they are intensifying over these two areas, therefore they manifest a kind of quasi-stationary component to favor the 'dipole' structure. Whereas the disturbances weaken and speed up over the eastern Pacific cold water region due to the interaction of sensible heating and evaporation with perturbational wind. Therefore the two major centers just show out-of-phase oscillation during one cycle around the latitudinal belt.

By introducing the SST anomalies in El Niño and La Niña years into the surface temperature, we also show that they have significant influence on LFO processes. In an anomalously warm year, the LFO disturbances dissipate more slowly over the central-eastern Pacific region and can travel further eastward; whilst in an anomalously cold year, the opposite is true.

Key words: Low frequency oscillation, Convective seesaw, Tropical model

I. INTRODUCTION

The general circulation shows intraseasonal oscillation with periods shorter than seasonal variations, among them a major component is those with periods between 30 to 60 days (LFO thereafter). In recent years, several works laid stress on its longitudinal-dependent features in addition to the propagating-wave character. Rui and Wang (1990) documented the development characteristics and dynamical structure of the LFO and proposed a four-stage life cycle of the disturbances: (1) initiation from tropical Africa and western Indian Ocean; (2) development and rapid intensification when travelling eastward over Indian Ocean; (3) weaken temporarily over Indonesia maritime continents and reintensify when migrating over western Pacific; (4) dissipate or emanate to extra-tropical region when they travel across the dateline. Zhu and Wang (1993) found that the tropical Indian and western Pacific oceans are

two prominent action centres for low-frequency convective variability. When convection is enhanced over Indian Ocean, the western Pacific often experiences an abnormally dry condition, whereas the development of convection over the tropical western Pacific tends to be accompanied by suppressed convection over the Indian Ocean. This convection seesaw is a fundamental characteristic of the LFO, as given in fig.1. They raised the question of what is the physical mechanism responsible for this strong regional standing oscillation pattern and suggested that it may be related to the land-sea contrast and sea surface temperature (SST) distribution. It is also noticed that the speed of eastward propagation of the disturbances is not uniform. They slows down when they intensify from the Indian Ocean to the western Pacific and speed up when they weaken over other areas in a latitudinal circle.

Several theoretical works on LFO also investigated the impact of the Indian-western Pacific warm waters on the development of disturbances. Miyahara (1987) introduced ideal zonal variation of convective heating strength in his multi-level model. Whereas Sui and Lau (1989) adopted the ideal two-dimensional distribution of SST. Both of them found that the disturbances intensify over warm water, dissipate when they move across cold waters, and become active again as they travel back to warm water regions. However the two models have simulated neither the twice-intensification over the Indian Ocean and western Pacific nor the dipole structure.

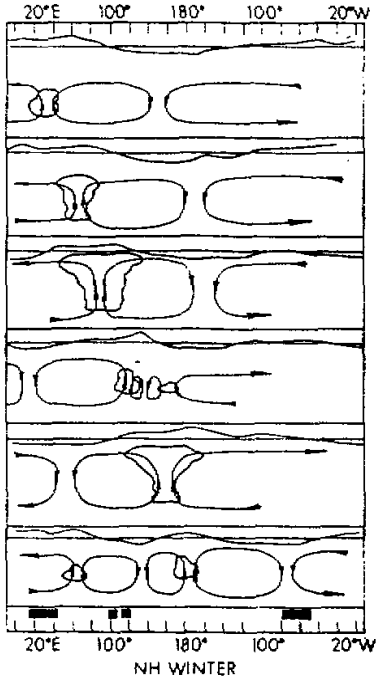

Fig.1. Schematic models of the tropical LFO on the equatorial zonal plane for boreal winter. The curves above the convection anomalies are velocity potential anomalies at 200 hPa with positive value denoting divergence (after Zhu and Wang, 1993).

The SST in the tropical Pacific Ocean shows strong intraseasonal variability with the 2~7 years El Niño and La Niña cycle as the most significant signal. They have strong impact on the tropical general circulation. Lau et al. (1986) found from the analysis of OLR data that LFO has some relationship with ENSO events and suggested that the LFO disturbances over the western Pacific may trigger ENSO events, and the latter may in turn influence the amplitude of LFO. From the longitude–time diagrams in Rui and Wang (1990) which shows the propagation of LFO from 1975–1977 and 1979–1985, it is also seen that there are obvious differences between abnormally warm and cold years. In a normal year, the convective activities are relatively weak over the eastern Pacific in autumn and winter, and the LFO disturbances normally only propagate to the dateline. During an ENSO event, the disturbances not only are stronger, but also travel further eastward to 160°W~ 140°W, thus enhance the convective activities over the eastern Pacific. Whereas during an La Niña event, the disturbances migrate to at most 160°E, there is almost no convective activity over cold water regions. So far we have not seen any model and theoretical research in this respect yet.

So in this paper, firstly we developed a simplified dynamic model which includes: (1) the interaction of condensational heating with flow field; (2) the feedback of sensible heating and evaporation on perturbational wind and (3) the zonal non–uniformity of the underlying surface and realistic SST distribution. It is used to simulate the propagation and development processes of LFO and the dipole structure related to the transition of circulation between each phases of the oscillation. Then we are to introduce the SST anomalies in El Niño and La Niñ a years into the above–mentioned model and discuss their impact on LFO processes.

II. DYNAMIC MODEL

The model used in this work is a two–layer β–plane linear one for tropical atmosphere. After adding and subtracting, respectively the u and v equations for the two layers and assuming no divergence for the vertically integrated wind (barotropic mode), we come to the set of equations which only includes baroclinic modes:

$$\begin{cases} \dfrac{\partial u}{\partial t} - \beta y v = -\dfrac{\partial \varphi}{\partial x} - \gamma u \ , \\ \dfrac{\partial v}{\partial t} + \beta y u = -\dfrac{\partial \varphi}{\partial y} - \gamma v \ , \\ \dfrac{\partial \varphi}{\partial t} + S\dfrac{(\triangle p)^2}{2} \ \nabla \cdot \vec{v} = -\dfrac{R}{C_p} \cdot \dfrac{\triangle p}{p_2} \ Q_2 \ , \end{cases} \tag{1}$$

where u、v and φ denote the difference of wind and potential height, respectively between the two layers, γ is the viscosity diffusion coefficient, S the static stability, Q_2 the heat forcing in the middle of the troposphere, C_p the specific heat of the air, R the thermodynamic constant, $\triangle p$ the pressure difference between the two layers. Here u、v and φ have the same (opposite) sign as those in the lower (upper) layer and are two times of their magnitude.

In order to calculate the convective condensational heating, we need an equation for water vapour. It is only written in the lower layer because the water content decreases exponentially with height. The linearized equation reads:

$$\frac{\partial q'}{\partial t} + \bar{q}_s \ \nabla \cdot \vec{v}/2 = -P + E' \ , \tag{2}$$

where P is precipitation, E' is perturbational evaporation rate, $\bar{q}_s$ the saturation

specific humidity of the lower layer, q' is the deviation from $\bar{q}_s$. Considering the difference of evaporation rate from land and ocean surface, we assume:

$$E' = \begin{cases} E_0' & \text{over oceans,} \\ E_0' \dfrac{W}{W_c} & \text{over lands .} \end{cases} \tag{3}$$

Where E_0' is the perturbational evaporation from ocean surface, W the moisture content of soil and W_c the soil moisture at saturation.

Over land, the evolution of W is determined by water budget:

$$\frac{\partial W}{\partial t} = P - E' . \tag{4}$$

Over the oceans, or when the predicted water content $W > W_c$, we assume $W = W_c$, the extra water is considered to be lost as runoff. W_c is set to be 10 g / cm^2.

The heat forcing term Q_2 in (1) consists of sensible heating Q_s' and condensational latent heating Q_L from convective activities:

$$Q_2 = Q_s' + Q_L .$$

A simple parameterization scheme is adopted for Q_L. The condensational heating is assumed to be proportional to the convergence of large-scale flow field, that is:

$$Q_L = L \cdot P . \tag{5}$$

The precipitation rate

$$P = \begin{cases} \dfrac{g}{\triangle p} E' - \eta q_s^* (\bar{T}_s) \nabla \cdot \vec{v} / 2 & \text{(when } \nabla \cdot \vec{v} < 0, \text{ and } q' \geqslant q_c) \\ 0 . & \text{(otherwise) ,} \end{cases} \tag{6}$$

where L is condensational potential heating, q_c is the specific humidity when precipitation begins. η is the parameter representing the strength of convection and is a constant here. It determines the efficiency of the transformation from converged water vapour to heat forcing. The factor $q_s^* (\bar{T}_s)$ is introduced into the coefficients to manifest the influence of underlying surface temperature on convective activities. It represents the saturation specific humidity at surface temperature $\bar{T}_s$. The higher the $\bar{T}_s$ is, the larger the $q_s^* (\bar{T}_s)$ value, and the more favourable for the convective activity.

For Q_s' and E_0', the aeronomic formulae are adopted. Following the parameterization of Emanuel(1987), linearizing about a basic state $\bar{U}_L$, we can get:

$$E_0' = -\rho C_q |\bar{U}_L| \, q' + \rho C_q \left(q_s^* - \bar{q}_s \right) \cdot sgn(\bar{U}_L) \cdot u / 2 , \tag{7a}$$

$$Q_s' = \rho C_H |\bar{U}_L| \left(T_s^* - T' \right) + \rho C_H (\bar{T}_s - \bar{T}) \cdot sgn(\bar{U}_L) \cdot u / 2 , \tag{7b}$$

where C_q、C_H are drag coefficients, q_s^* is the same as in (6), $\bar{T}_s$ the zonal mean of surface temperature, T is air temperature, $\bar{T}$ is its zonal mean value, T' is the perturbation of T calculated from φ in (1), $\bar{U}_L$ is the mean zonal wind in the lower layer, sgn($\bar{U}_L$) is the sign function of $\bar{U}_L$, it is positive in regions of mean westerlies and negative in mean easterlies.

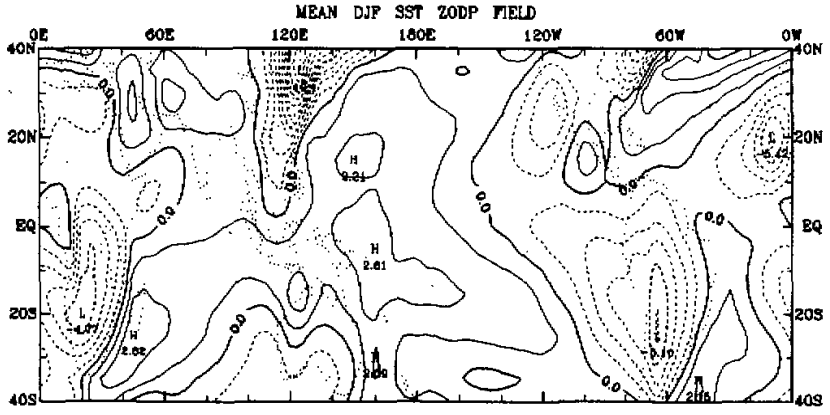

Fig.2. Zonal departure of surface temperature T_s^* in low latitudes for boreal winter.

This model includes two kinds of feedback processes, one is the CISK mechanism which is manifested in the second term in (6); the other is the mechanism of the interaction of sensible heating and evaporation with perturbational wind, which is manifested in the second terms in (7a) and (7b). These terms are positive when the perturbation wind is of the same sign with mean wind. This means that the perturbation wind coincides with the mean wind and enhances the sensible and latent heat flux; whereas when the perturbational wind is of opposite sign with the mean wind, they would cancel each other and reduce the heat and moisture flux.

The integrated region is the latitudinal circle between 42.5°N and 42.5°S. The staggered C–grid with spacing of 5° long. by 5° lat. is adopted for horizontal differencing. Time integration is semi–implicit scheme and central difference. In order to repress high–frequency oscillations, Euler scheme is used at the initial step and then repeatedly after certain steps.

To lay stress on the non–uniformity of the underlying surface, realistic land–sea distribution is introduced, and the zonal mean temperature is subtracted from underlying surface temperature field (T_s) for boreal winter in low–latitude to get its zonal departure T_s^*. Fig.2 shows the distribution of T_s^*. There is a high SST centre in the western Pacific, whilst the continents of Africa and South America are relatively cold. The Indonesia maritime continents are also colder than the surrounding waters. We shall see that this non–uniform distribution of underlying surface strongly regulates the propagation and development of LFO disturbances.

III. RESULTS of NUMERICAL EXPERIMENT

1. *The Propagation of LFO Disturbances*

Firstly, we analyze the time evolution of divergence and precipitation averaged from 2.5°N ~ 2.5°S to represent the situation at the equator. The evolutions of wind divergence and precipitation are shown in Figs.3a and 3b. When preparing these figures, the data have been subjected to time filtering, that is, the time mean value is subtracted from the time series for each grid, then the new series is undergone 5–day running mean to eliminate high–frequency components (shorter than 10 day period) of the deviation from time mean.

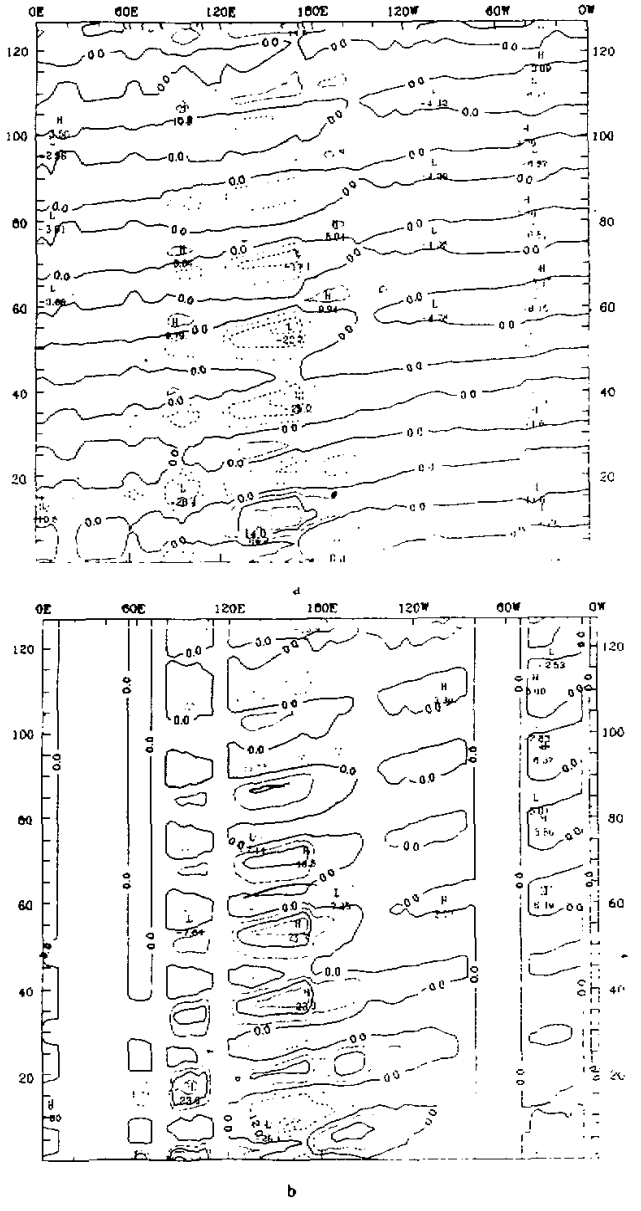

Fig.3. Time evolution for anomalies in (a) divergence and (b) precipitation at the equator. Solid (dashed) contours denote positive (negative) value.

This applies to all the longitude–time diagrams in this paper.

From Figs.3a and 3b, we can see that the evolution of precipitation corresponds well to that of wind divergence. The convergence centre (strong precipitation region) originates over the western Indian Ocean near 60°E, then it propagates eastward to about 90°E and at the same time grows in strength until it reached the maritime continents, where the convergence centre weakens and the associated precipitation even stops temporarily. After that, the disturbances continue to travel eastward and reintensify over the western Pacific warm pool. When they get to the low SST region of the eastern Pacific, they dissipate very rapidly. However the disturbances can maintain themselves until they move to the east of Africa and become active again over the Indian Ocean. Then they weaken over maritime continent, redevelop over the western Pacific and repeat the above cycle periodically. Everytime the disturbances traverse the whole latitudinal circle, they undergo twice intensification over the Indian and western Pacific Ocean. This cyclic behavior is very clear until more than 100 days. Unlike the continuous movement of divergence, the migration of the convective precipitation shows a kind of discontinuity which is consistent with observations.

As the disturbance centres move eastward continuously, locally we observe that the convergence and divergence oscillate with time. There are two prominent oscillation centres over Indian Ocean and western Pacific, respectively. The period is about 20 days, shorter than that of observed.

We have adjusted the parameter η in (6) and found that when the condensational heating is stronger, the wave speed is further reduced and the period is more realistic. This further confirmed that the CISK mechanism may reduce the speed of disturbances.

Interestingly, the disturbances propagate more slowly over western Pacific warm pool than from the eastern Pacific to Africa. From the Indian Ocean to western Pacific, it is about 14 longitude / day whilst over other regions, it is around 19 longitude / day. Observations show that the disturbances do slow down over warm waters when they grow in strength and speed up when they weaken. Our results correspond qualitatively with that.

The non–uniformity of the movement of disturbances is the result of the interaction of internal dynamics with non–uniform external forcing. Over the western Pacific warm pool, there is very active convection, the interaction of convective heating with large–scale flow field slows down the wave speed. For theoretical analysis please refer to Yang and Zhu (1990). Over the relatively colder eastern Pacific where convection is suppressed, the effect of condensational heating is not very important and it is the feedback of evaporation and sensible heating with perturbational wind which maintains the eastward propagation of the disturbances. The works of Emanuel (1987) and others have shown that this mechanism favours the eastward movement of disturbances. Therefore, their phase speed is faster over the eastern Pacific. This explains the zonal non–uniformity of the phase speed of LFO. This in turn causes the out–of–phase oscillation of the two major centres because the time it takes the disturbances to travel from the Indian Ocean to the western Pacific is about the same as that to traverse the remaining part of the latitudinal circle.

2. *Periodical Evolution of the Circulation and the Dipole Structure*

We now analyze the evolution of circulation in a LFO cycle. One cycle of the LFO is divided into 5 phases. Fig.4 shows the two–dimensional distribution of divergence in each of the phases.

Phase 1: On model day 10 (Fig.4a), there is a large divergent region from the northern Indian Ocean to west of the dateline in the Pacific with a center north of the equator in the

western Pacific. The eastern Pacific to Atlantic Ocean region is dominated by convergence whose center is much weaker than the divergence center. Notice that there is a small convergence center over the southwestern Indian Ocean near 15°S, 55°E, which has been there for several days.

Phase 2: The above–mentioned small convergence center grows in strength and expands in northeast direction. By day 14 (Fig.4b) a large convergent region is formed over the Indian Ocean with two centres over 60°E and 90°E, respectively near the equator. The latter center is stronger. Meanwhile, the divergence region over the western Pacific expands and its center moves eastward to 160°E. The phase of this center is opposite to the convergence center over the Indian Ocean and together they form a kind of dipole structure.

Phase 3: At day 20 and 21 (Fig.4c), the disturbance moves from the Indian Ocean to western Pacific warm pool and grows into a strong convective center. The divergence center over the western Pacific in Phase 2 now moves eastward and weakens in strength. Another divergence center migrates from Africa to the western Indian Ocean and suppresses the convergence there. Notice that the convergence over Indonesia is weak all the time, indicating that this region is not favorable for convections to develop.

Phase 4: At day 23 (Fig.4d), most of the Indian Ocean is dominated by divergence while there is a strong convergence center over the western Pacific at about 160°E near the equator. The two centres again formed a dipole structure, but with reversed polarity to that of Phase 2 in day 14, although the divergence center is relatively too weak.

Phase 5: At day 25 (Fig.4e), the divergence and convergence centres north of the equator are strengthened. The pattern suggests a kind of energy dispersion from the equator to northeast and southeast by Rossby waves.

At day 27, (Fig.4f), the divergence center at the western Pacific intensifies and expends whereas the convergence to the east weakens and moves eastward. The region from the northern Indian Ocean to western Pacific is again dominated by divergence. This pattern resembles that of day 10.

From Phase 1 to Phase 5, the evolution of divergence field undergoes a complete cycle. The divergence and precipitation repeat the five phases periodically thereafter. For example, on day 30 (Fig.4g), the patterns are very much like that of Phase 2 of day 14. Day 56 (Fig.4h) represents Phase 4, the dipole structure is very clear and with opposite polarity to that of day 30.

It is seen that during this periodical evolution, the most prominent feature is the two strongest oscillation centres at the Indian Ocean and western Pacific Ocean. Their seesaw oscillations give rise to the dipole structure in divergence field. It means that when convection is active over the Indian Ocean, the western Pacific experiences an abnormally dry spell and the convective activities are suppressed; whilst when convection increases over the western Pacific, the Indian Ocean normally is dominated by lower–level divergence and downward motion. The maritime continents, where the smallest convective variability is observed, is a nodal point between them.

Our results are in reasonable agreement to the observational analysis by Rui and Wang (1990) and by Zhu and Wang (1992) (see Fig.1). The former revealed the four stage evolution of the LFO disturbances, whereas the latter laid stress on the seesaw oscillation between the two centres. Their analyses and our results both suggest that this is the result of twice–development and intensification of disturbances over the Indian Ocean and western Pacific warm

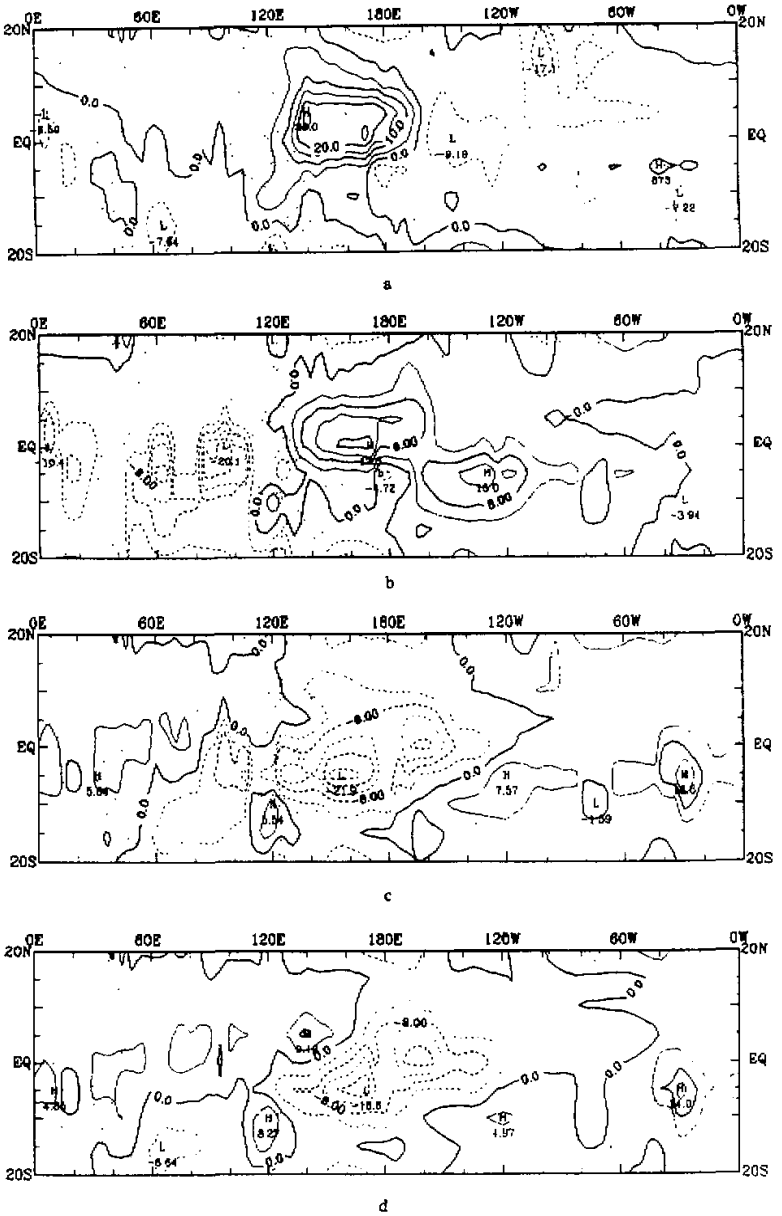

a

b

c

d

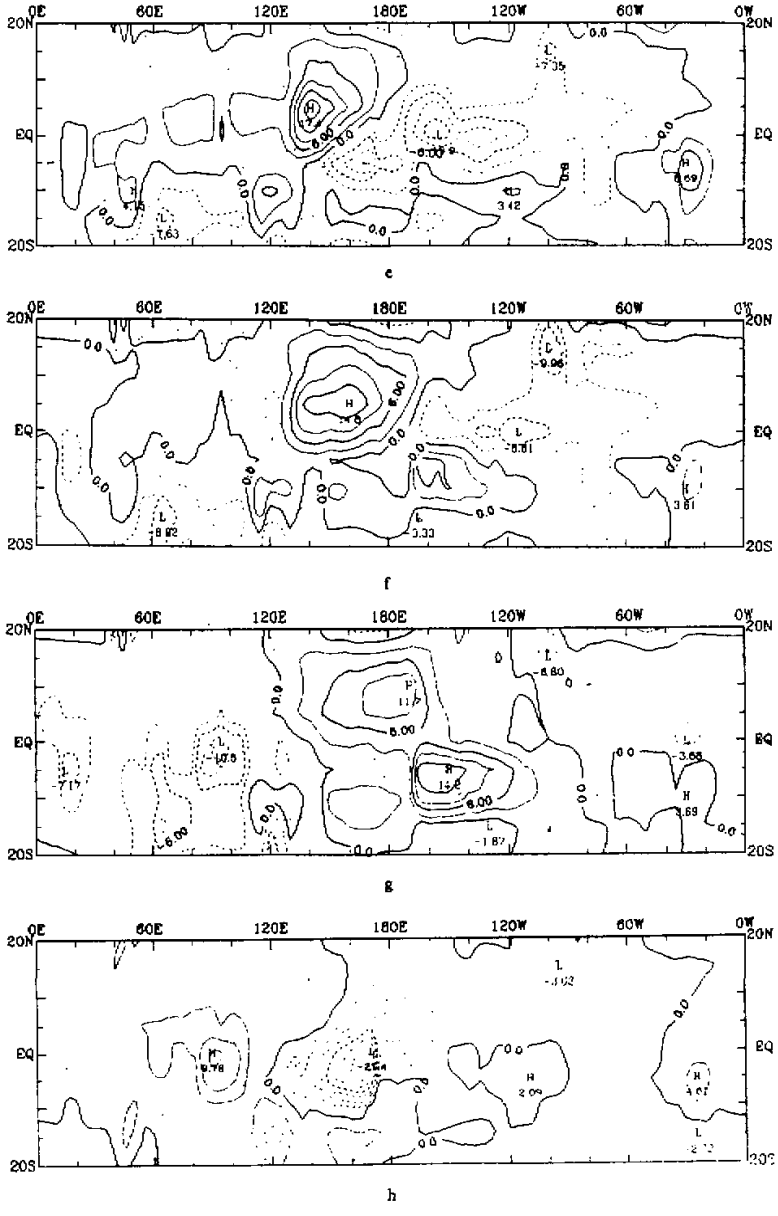

Fig.4. Evolution of divergent field in one LFO cycle.

a. Phase 1 (day10) b: Phase 2 (day14) c: Phase 3 (day21) d: Phase 4 (day23)

e: Phase 5 (day25) f: Phase 1 (day27) g: phase 2 (day30) h: Phase 4 (day56)

pools. In these two areas, the strong fluxes of sensible and latent heat from the ocean as well as the interaction of condensational heating with large-scale flow favour the development of convective activities. In contrast, disturbances weaken or dissipate over Indonesia maritime continents due to suppressed sensible heating and evaporation there. This demonstrated the strong regulating effect of the thermal non-uniformity of the underlying surface on the propagation and development of disturbances in tropical atmosphere. The collective behavior of many individual eastward-moving events contributes to the formation of the seesaw in boreal winter. The model results strongly support Zhu and Wang's (1993) idea that the propagating low frequency convective systems and convection seesaw should be regarded as two aspects of a unified phenomenon.

To our knowledge, none of the previous works on the mechanism of LFO has explained the twice-enhancement or simulated the phase-transition of LFO processes. Because our model incorporates the detailed land-sea contrast and two-dimensional distribution of SST, it reproduces the processes reasonably well. Sui and Lau (1989) and Miyahara (1987) stressed the importance of the non-uniformity of SST in regulating the amplitude of disturbances. They gave idealized SST distribution which influences precipitation through (6). In their models, T_s is a function of longitude as well as latitude. Higher T_s means larger $q_s^*(T_s)$, larger moisture convergence and stronger condensational heating. Therefore, the disturbances tend to develop over warmer waters and dissipate over colder waters. But in our model, $\overline{T}_s$ in (6) is the zonal mean value. So the zonal non-uniformity of SST influences the development of disturbances through another mechanism, i.e., through zonally differential sensible heating and evaporation. This produces a background convergence and upward motion over warm waters, which is favorable for the development of disturbances, then they further grow by the feedback of convective heating with large-scale flow. On the contrary, over cold waters and dry continents, the heat and moisture flux from surface are suppressed, so that convective activities tend to weaken or dissipate. In this way, the disturbances select their preferred locations for development.

IV. LFO IN EL NIÑO AND LA NIÑA YEARS

In this section, we introduce SST anomalies in El Niño and La Niña years, respectively into the model and analyze their influence on LFO processes. The SST anomaly in El Niño years is taken from the mature phase of Rasmusson and Carpenter (1982)'s analyses and that in La Niña years is assumed to be of the same distribution but in opposite sign with that in El Niño years.

1. *LFO in El Niño Years*

Fig.5a is the model result of time evolution of precipitation in an El Niño year. Comparing it with Fig.3b of a normal year, we can see that the longitude at which the disturbances reach their strongest phase in Fig.5a is to the east of the corresponding centres in Fig.3b and the dissipation is slower after the disturbances travel to the east of the dateline. After day 35, there maintains a weak oscillation center between 140°W and 160°W in eastern Pacific. The disturbances travel much further eastward in Fig.5a than in Fig.3b, so the convective activities in the eastern Pacific are enhanced in an ENSO year than in a normal year.

2. *LFO in La Niña Years*

Fig.5b is the same as Fig.5a but for a La Niña year. This figure is also quite different

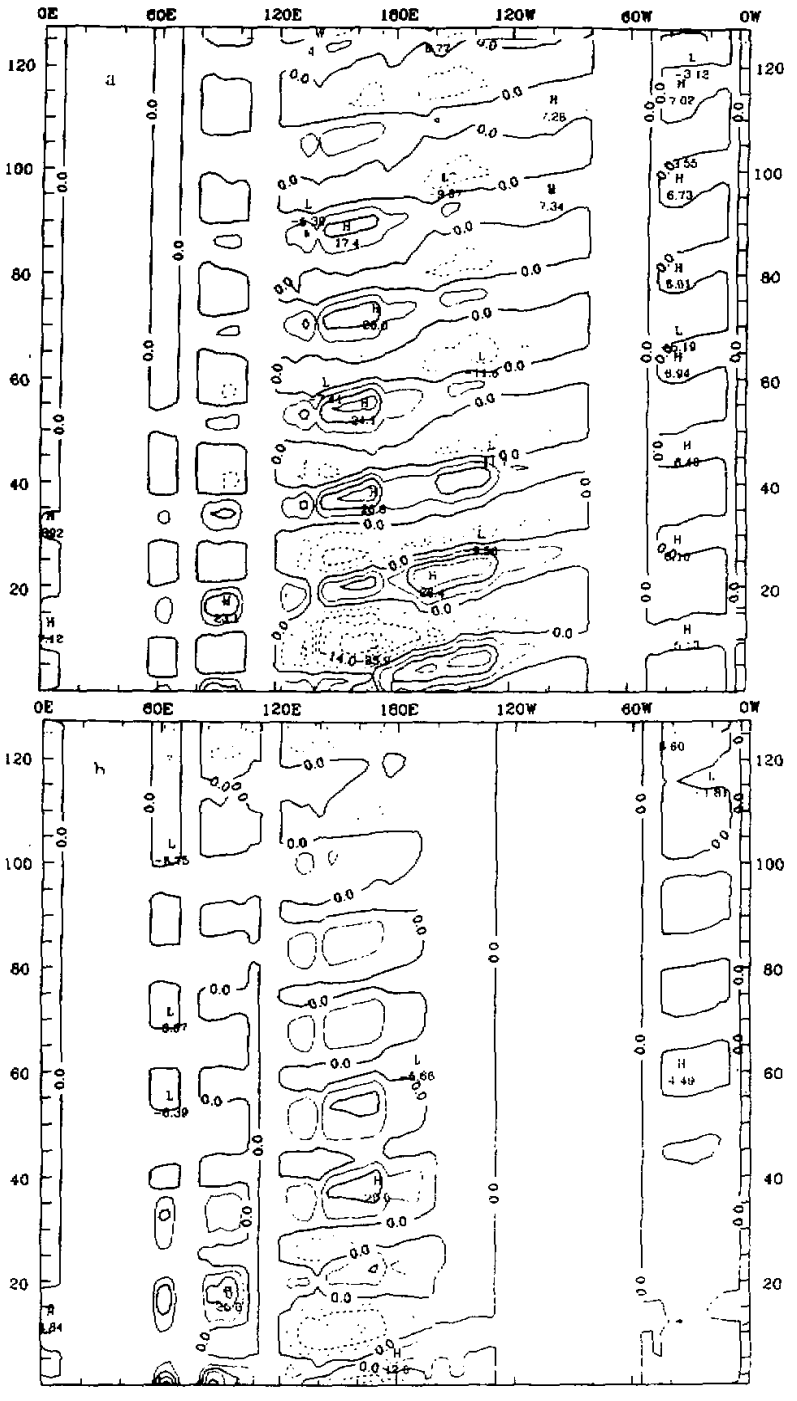

Fig.5. Time evolution of precipitation in (a) El Niño years and (b) La Niña years

from Fig.3b in that there is no significant eastward propagation of the convective centers and their dissipation is very rapid, so there are almost no convective activities in the eastern Pacific Ocean.

Comparing Fig.5a and Fig.5b, the contrast is even sharper. The systematic eastward propagation in Fig.5a disappears in Fig.5b. This is because in El Niño years, the zonal SST temperature gradient in the Pacific Ocean is weaker, so that the Walker circulation is weaker. This favours the eastward propagation of disturbances and the development of convections in the eastern Pacific. On the contrary, in La Niña years, the SST gradient is stronger and the eastern Pacific is dominated by downward motion. This prohibits the eastward propagation of convective activities. Our results demonstrate that the SST anomalies not only influence the general circulation of tropical atmosphere, but also have significant impact on the development and propagation of its LFO processes.

V. SUMMARY

In this work, a tropical β-plane model with realistic zonally non-uniform surface temperature and land-sea distribution is developed which incorporates the wave-CISK mechanism as well as the interaction between sensible heating and evaporation with perturbational wind. Using this model, the tropical 30~60 day LFO processes are simulated with emphases on the seesaw oscillation and dipole structure between the Indian and western Pacific oceans.

The model reproduced the initiation of disturbances over the eastern Africa and western Indian Ocean, their growth over the Indian Ocean as they propagate eastward, their temporal dissipation over Indonesia maritime continents and reintensification over the western Pacific warm pool. Moreover, it simulated the dipole structure caused by the seesaw oscillation of the two active centres over the Indian Ocean and western Pacific Ocean, respectively.

The dipole structure is the result of the interaction of non-uniform external forcing from underlying surface with internal dynamics of the tropical atmosphere. It is the collective behavior of the longitudinal-dependent evolution of eastward-moving low frequency convective systems that is responsible for the formation of seesaw. Over the Indian Ocean and western Pacific warm pool, strong sensible heating and evaporation as well as the CISK mechanism caused the twice-intensification of disturbances, so there formed two active oscillation centres. Whilst over the maritime continents and the eastern Pacific cold water regions, the disturbances tend to weaken or dissipate. On the other hand, the propagation speed of disturbances is not uniform in a latitudinal circle and shows a stationary component between the Indian Ocean and western Pacific warm pool. The out-of-phase enhancement betweem the two centres gives rise to the dipole structure. This is bacause over the warm waters where the disturbances grow, the wave-CISK mechanism slows down the speed of the eastward propagating waves, whereas over eastern Pacific, the feedback of sensible heating and evaporation on perturbational wind is very important in maintaining the eastward migration of perturbations and it fastens the wave speed. So it takes about the same time for the disturbances to travel from the Indian Ocean to the Western Pacific as it traverse the remaining part of a latitudinal circle.

By introducing the SST anomalies into the surface temperature, we also show that the SST anomalies in El Niño and La Niña years have significant influence on the LFO processes. In an anomalously warm year, the LFO disturbances dissipate more slowly and can travel eastward all the way to the eastern Pacific; whilst in an anomalously cold year, the oscillation weakens more rapidly and the eastward propagation is prohibited.

Our simulation has some discrepences as compared with the observations. For example,

the transition phases between the two phases of the dipole are not very well simulated and the divergence center over the western Pacific is displaced somewhat northward. Further improvement is needed in parameterization of convective activities and land surface processes.

REFERENCES

Emanuel, K. A. (1987), An air–sea interaction model of intraseasonal oscillations in the tropics, *J. A. S.*, **44:** 2324–2340.

Lau, K. –M., and L. Peng, (1986), The 40～50 day oscillations and the El Niño Southern Oscillaton: A new perspective, *Bulletin* A. M. S., **67:** 533–534.

Miyahara, S. (1987), A simple model of the tropical intraseasonal oscillations. *J. Meteo. Soc. Japan*, **65:** 341–351.

Rasmusson, E. M., and T. H. Carpenter (1982), Variations in tropical sea surface temperature and surface wind fields associated with the Southern Oscillation / El Niño. *Mon. Wea. Rev.*, **110:** 354–384.

Rui, H–L., and B. Wang (1990), Development characteristics and dynamic structure of tropical intraseasonal convection anomalies. *J. A. S.*, **47:** 357–379.

Sui, C. H. and K. –M. Lau (1989), Origin of low–frequency (intraseasonal) oscillations in the tropical atmosphere, Part II: Structure and propagation of mobile wave–CISK modes and their modification by lower boundary forcings. *J. A. S.*, **46:** 37–56.

Yang, Y. and B. –Z. Zhu (1990), Interaction between waves in low–latitude atmosphere and tropical low–frequency oscillation. *Acta Meteoreologica Meteo. Sinica*, **4:** 629–639.

Zhu, B. –Z. and B. Wang (1993), The 30–60–day convection seesaw between the tropical Indian and western Pacific Oceans. *J. A. S.*, **50:** 184–199.